SYNERGIZING DYNAMIC SCORE AGGREGATION WITH CONTRASTIVE REGULARIZATION FOR OPEN-SET SEMI-SUPERVISED OUT-OF-DISTRIBUTION DETECTION

Anonymous authorsPaper under double-blind review

000

001

002

004

006

008 009 010

011 012

013

014

016

017

018

019

021

023

025

026

027

028

029

031

032

034

037

038

040

041

042

043

044

046

047

048

052

ABSTRACT

Semi-supervised learning (SSL) has achieved remarkable progress by leveraging both limited labeled data and abundant unlabeled data. However, unlabeled datasets often contain out-of-distribution (OOD) samples from unknown classes, which can lead to performance degradation in open-set SSL scenarios. Current approaches primarily address this issue by identifying outliers through OOD detection. Yet, methods relying solely on neural networks are constrained by the absence of labeled OOD samples for supervision. To overcome this limitation, we propose a novel open-set OOD detection framework named **SDM**, which **S**ynergizes Dynamic Score Aggregation (DSA) and Matrix Contrastive Regularization (MCR). Specifically, we formulate OOD detection as a semi-unbalanced optimal transport (SemiUOT) problem and derive pseudo-labels by solving it. The DSA module dynamically converts SemiUOT into a classical optimal transport (OT) formulation. Unlike existing OT-based methods, DSA provides theoretically grounded and more accurate pseudo OOD scores while avoiding the direct computation of the transport plan. Meanwhile, the MCR module enhances feature discrimination through contrastive learning, thereby improving overall performance. Empirical results demonstrate the superiority of SDM. Additionally, we conduct extensive analytical experiments to elucidate the properties of each component.

1 Introduction

Semi-supervised learning (SSL) is a pivotal machine learning paradigm that leverages abundant unlabeled data alongside limited labeled data (Xiao et al., 2024; Berthelot et al., 2019; Zheng et al., 2022; Kingma et al., 2014; Chen et al., 2024; Yang et al., 2024; Min et al., 2024). Traditional SSL relies on the assumption that both labeled and unlabeled data share the same class space and distribution (Li et al., 2023). However, this closed-world setting is often unrealistic. In real-world open-set SSL scenarios, unlabeled data frequently contain out-of-distribution (OOD) samples from unknown classes, which can severely degrade model performance if not properly handled.

To alleviate this problem, researchers begin to explore the identification of outliers (Qin et al., 2024; Shen et al., 2024; Kaushik et al., 2024), namely OOD detection. While one possible solution is to directly implement OOD detection during testing (Hendrycks & Gimpel, 2016; Liu et al., 2020; Huang et al., 2021b; He et al., 2022; Ma et al., 2023), this approach only considers the testing phase with the model trained on purely in-distribution (ID) data. In open-set SSL, the model must be jointly optimized on both labeled and unlabeled data while ensuring the OOD detection module learns effectively without compromising classification accuracy. Consequently, (Yu et al., 2020b; Guo et al., 2020) propose to integrate OOD detection with semi-supervised learning during the training phase. However, the absence of reliable OOD labels hinders effective learning and the joint optimization framework risks sacrificing closed-set classification accuracy.

To address this challenge, recent works (Saito et al., 2021; Ren et al., 2024) introduce third-party proxies into the training phase. For instance, (Saito et al., 2021) employs a one-vs-all (OVA) classifier for OOD detection. However, this method requires training a separate classifier for each known class, which is computationally inefficient. Although (Ren et al., 2024) proposes to train a neural binary classifier using pseudo OOD scores obtained through entropy-regularized optimal transport (OT), the

entropy regularization can compromise label accuracy, and the practice of artificially amplifying the weights of unlabeled samples lacks a theoretical foundation.

To resolve this dilemma, we model the OOD detection task as a semi-unbalanced optimal transport (SemiUOT) problem and propose a **dynamic score aggregation** (DSA) module. DSA dynamically converts the SemiUOT problem into classical OT, eliminating the need for entropy regularization or ad-hoc weight amplification. This allows it to produce more accurate pseudo OOD scores for supervising the neural binary classifier. Furthermore, we introduce a **matrix contrastive regularization** (MCR) module, which enhances feature discrimination through contrastive learning without incurring inference-time overhead. Integrating these components, we propose **SDM**, a novel open-set semi-supervised OOD detection framework that **S**ynergizes **D**SA and **M**CR. Extensive experiments demonstrate the superiority of SDM over existing methods.

The main contributions are listed as follows:

- We innovatively propose the DSA module, which dynamically converts the SemiUOT problem into classical OT. This theoretically grounded approach yields more accurate pseudo-labels efficiently, overcoming key limitations of existing OT based methods. Furthermore, we introduce a fast approximation algorithm for DSA with a theoretically analyzed error bound.
- We design the MCR module as an auxiliary task based on self-supervised learning. MCR enhances feature discrimination without introducing inference latency. Integrating DSA and MCR, we construct SDM, a novel framework that synergistically combines OT with self-supervised regularization for open-set semi-supervised OOD detection.
- Extensive experiments on benchmark datasets demonstrate that SDM achieves competitive, and often superior, performance compared to state-of-the-art methods. Additional ablation and analytical studies provide insights into the properties and individual contributions of each component.

2 Related works

2.1 OPTIMAL TRANSPORT

OT quantifies the discrepancy or distance between two distributions by calculating the minimum transport cost (Khamis et al., 2024). As a mathematical tool, recent advances have shown the promising potential of OT for various machine learning tasks, such as natural language processing (Cheng et al., 2024a; Sun et al., 2023; Cheng et al., 2024b), computer vision (Li et al., 2025; Lin & Chan, 2023; Izquierdo & Civera, 2024; Chowdhury et al.), graph matching and representation (Maretic et al., 2022; Zeng et al., 2023; 2024), generative models (Tong et al., 2023a;b; Li et al., 2024; Hui et al., 2025; Choi et al., 2023), and reinforcement learning (Klink et al., 2024; Asadulaev et al., 2024; Sun et al., 2025). Classical OT is the most basic form of OT theory, where both marginal equality constraints on source and target distributions are preserved.

Definition 2.1 (Classical OT). Given two distributions α and β , each containing M and N units, α and α are the weights vectors of them, and α is the transport cost matrix. The classical OT is to find the optimal transport plan $\alpha \in \mathbb{R}^{M \times N}_+$ in the feasible solution set α .

$$\min_{\boldsymbol{\pi} \in \Pi(\boldsymbol{\alpha}, \boldsymbol{\beta})} \langle \mathbf{C}, \boldsymbol{\pi} \rangle_F, \Pi(\boldsymbol{\alpha}, \boldsymbol{\beta}) := \left\{ \boldsymbol{\pi} \in \mathbb{R}_+^{M \times N} : \boldsymbol{\pi} \mathbf{1}_N = \boldsymbol{a}, \boldsymbol{\pi}^{\mathrm{T}} \mathbf{1}_M = \boldsymbol{b} \right\}.$$
 (1)

Since classical OT is essentially a linear optimization process, it can be solved exactly using any linear solver. However, when trying to make OT work in the real world, things are often trivial. If one of the two marginal constraints is relaxed, SemiUOT is defined as follows.

Definition 2.2 (SemiUOT with KL-Divergence). *SemiUOT is to find the optimal transport plan when the target constraint on the source distribution is removed (Le et al., 2021), the formulation is,*

$$\min_{\boldsymbol{\pi} \in \Pi(\boldsymbol{\alpha}, \boldsymbol{\beta})} \langle \mathbf{C}, \boldsymbol{\pi} \rangle_F + \tau_a \mathit{KL}(\boldsymbol{\pi} \mathbf{1}_N \| \boldsymbol{a}), \Pi^s(\boldsymbol{\alpha}, \boldsymbol{\beta}) := \left\{ \boldsymbol{\pi} \in \mathbb{R}_+^{M \times N} : \boldsymbol{\pi}^{\mathrm{T}} \mathbf{1}_M = \boldsymbol{b} \right\}, \tag{2}$$

where τ_a is the weight parameter. The divergence term KL is used to measure the discrepancy between the marginal distribution of the transport plan and the source distribution.

A common approach to SemiUOT involves introducing an entropy regularization term and solving the resulting objective with a Sinkhorn-like algorithm (Cuturi, 2013), which may compromise accuracy.

2.2 RELATIONS BETWEEN OOD DETECTION AND OPTIMAL TRANSPORT

The motivation for the OT-based OOD detection is intuitive. For the probability distribution of both the source and the target domain (e.g., the feature embedding of unlabeled and labeled data), the common assumption is that they both obey the uniform discrete distribution. If we model OOD detection problem as classical OT on this basis, it is difficult to distinguish ID samples from OOD samples via the transport plan π . Thus, (Ren et al., 2024) enlarges the weights of the unlabeled data to force the marginal constraint of target domain (i.e., $\pi^T \mathbf{1}_N = a$) to be relaxed. The probability that the sample with less total transmission quality is an OOD sample is greater, and vice versa. Then, the pseudo OOD score obtained via the OT module can be computed as, $\mathbf{S} = \frac{1}{k} \pi \mathbf{1}_N$, assuming that the target domain is the feature embedding of unlabled data. Due to the mechanism above, it is unrealistic to deploy it directly during testing. A more practical approach is to use \mathbf{S} as the labels to train the neural OOD detector. However, the redundant mass k based OOD detection lacks theoretical support and the common Sinkhorn-like OT solvers risk producing unreliable pseudo OOD score. In this paper, we directly model the OOD detection task as SemiUOT and tackle it in a more accurate way.

2.3 Self-supervised regularization for semi-supervised learning

Common SSL strategies are pseudo-labeling and consistency regularization (Sohn et al., 2020; Li et al., 2022b;a; Sosea & Caragea, 2023; Ihler et al., 2024). Slightly different from SSL, the data for self-supervised learning is all unlabeled (Grill et al., 2020; Zbontar et al., 2021; Zhang et al., 2023; Lu et al., 2024; Zhang et al., 2024). Interestingly, when self-supervised learning is used as an auxiliary task for representation learning, performance improvement of semi-supervised learning can be observed (Zhai et al., 2019). For example, (Lee et al., 2022) addresses the inefficiency of traditional consistency regularization strategies in SSL by leveraging the contrastive learning mechanism of unlabeled data. (Li et al., 2021) proposes contrastive graph regularization to jointly optimize class probabilities and low-dimensional embeddings. Whether such strategy is effective in OOD tasks is still an underexplored research topic. Based on contrastive learning, we design the MCR module to further boost the performance of the model.

3 METHODOLOGY

3.1 Problem Definition

Source and target domain sample: The source domain sample $\mathbf{X}_u \in \mathbb{R}^{M \times H \times W \times CH}$ is composed of unlabeled data with known classes and unlabeled data with unknown classes (i.e., OOD sample), where M is the batch size of the source domain sample and H,W,CH are the height, width and number of channels of the input image date respectively. The target domain sample is the labeled data $\mathbf{X}_l \in \mathbb{R}^{N \times H \times W \times CH}$ with known classes, where N is the batch size of the target domain sample. Both the labeled sample and the unlabeled sample with known classes are called ID sample. Note that M should be larger than N to comply with the setting of open-set SSL.

Open-set semi-supervised OOD detection: Given \mathbf{X}_u and \mathbf{X}_l , the open-set semi-supervised OOD detection is to detect OOD samples in \mathbf{X}_u with \mathbf{X}_l as a reference and perform semi-supervised learning over both \mathbf{X}_u and \mathbf{X}_l . This paper focuses on training neural networks to predict the OOD probability $\hat{\mathbf{S}} \in \mathbb{R}^{M+N}_+$ under the supervision of pseudo labels obtained by OT and preserving the closed-set classification accuracy through self-supervised regularization.

3.2 Overview

As shown in Figure 1, SDM is composed of three modules, namely the semi-supervised learning module, the OOD detection module, and the MCR module. The closed-set classification module g adopts the same architecture as (Sohn et al., 2020; Ren et al., 2024). For a batch of sample from \mathbf{X}_u and \mathbf{X}_l , we perform weak augmentation once and strong augmentation twice on \mathbf{X}_u to obtain $\mathbf{X}_w, \mathbf{X}_s^1, \mathbf{X}_s^2 \in \mathbb{R}^{M \times H \times W \times CH}$. The specific augmentation method is consistent with (Sohn et al., 2020). The augmented source and target sample are mapped to their feature embedding $\mathbf{Z} = f(\mathbf{X}) \in \mathbb{R}^d$ through feature encoder f, where d is dimension of feature embedding. The pseudo

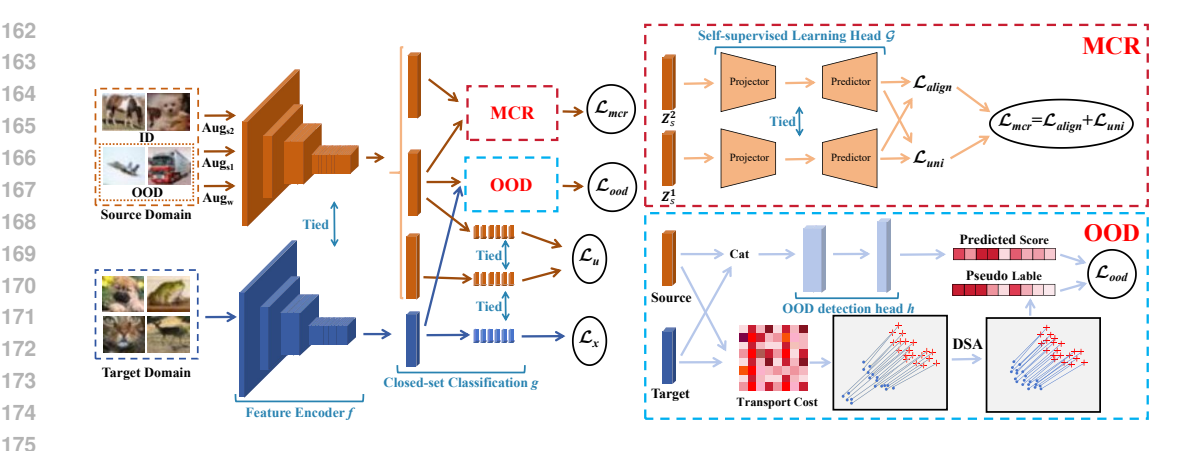


Figure 1: The left part of the figure depicts the overall framework of SDM and the right part of the figure shows the details of the MCR (top) and DSA (bottom) module."Tied" indicates weight sharing.

OOD scores S of the unlabeled samples are estimated by the DSA module and OOD loss is,

$$\mathcal{L}_{ood} = \frac{1}{M+N} \|\hat{\mathbf{S}} - \mathbf{S}'\|_2^2, \tag{3}$$

where $\hat{\mathbf{S}} = h(\mathbf{X}_l \oplus \mathbf{X}_w)$, $\mathbf{S}' = \mathbf{S} \oplus \mathbf{1}_N$ and \oplus indicates the concat operation. By computing the weighted sum of alignment loss and uniformity loss between \mathbf{X}_s^1 and \mathbf{X}_s^2 as \mathcal{L}_{mcr} , the MCR module works as an auxiliary task to enforce the feature encoder to learn better embedding. Putting all of these together according to weight, the total loss is,

$$\mathcal{L} = \mathcal{L}_x + \mathcal{L}_u + \gamma_1 \mathcal{L}_{ood} + \gamma_2 \mathcal{L}_{mcr}, \tag{4}$$

where \mathcal{L}_x and \mathcal{L}_u are supervised loss and unsupervised loss in Fixmatch (Sohn et al., 2020), whose weight coefficients are γ_1 and γ_2 respectively. The detailed algorithm of SDM is shown in Section A.1.

3.3 DYNAMIC SCORE AGGREGATION

We propose the DSA approach to estimate pseudo OOD scores in a more accurate and efficient manner, supported by theoretical guarantees. To further accelerate the computation, we introduce a targeted approximation method. Theoretical analysis also establishes an approximation error bound.

Firstly, We adopt the formulation of SemiUOT as Equation (2) to model the OOD detection task as the SemiOT problem, where $\alpha = \sum_{i=1}^M \frac{1}{M} \delta_{\mathbf{u}_i}$, $\beta = \sum_{i=1}^N \frac{1}{N} \delta_{\mathbf{l}_i}$ are the distribution weight of source samples and target samples respectively, and δ is the Dirac function. Given the feature embedding of labeled sample \mathbf{Z}_l and that of strong augmented unlabeled sample \mathbf{Z}_s^1 , we calculate the transport cost from \mathbf{Z}_s^1 to \mathbf{Z}_l as $\mathbf{C} = \mathbf{1}_{M \times N} - \frac{\mathbf{Z}_s^1 \mathbf{Z}_l}{\|\mathbf{Z}_s^1\|_2 \cdot \|\mathbf{Z}_l\|_2}$. Then, instead of directly solving the SemiUOT problem via Sinkhorn-like approach, we have the following proposition to transform the SemiUOT problem to classical OT and the problem can be tackled in a more accurate and efficient way.

Proposition 3.1 (Dynamic Score Aggregation with Exact SemiUOT Solver). Given SemiUOT with KL-Divergence shown in Equation (2), we can rewrite its dual form as below:

$$\min_{\boldsymbol{u},\boldsymbol{v},\boldsymbol{s},\zeta} \mathcal{J} = \tau_a \left\langle \boldsymbol{a}, \exp\left(-\frac{\boldsymbol{u}+\zeta}{\tau_a}\right) \right\rangle - \langle \boldsymbol{v}-\zeta, \boldsymbol{b} \rangle, s.t.u_i + v_j + s_{ij} = C_{ij}, s_{ij} \ge 0, \quad (5)$$

where u, v, s, and ζ are dual variables. Equation (5) can be rewritten as classical OT:

$$\min_{\boldsymbol{\pi} \geq 0} \mathcal{J}_{S} = \langle \boldsymbol{C}, \boldsymbol{\pi} \rangle, s.t. \boldsymbol{\pi} \mathbf{1}_{N} = \boldsymbol{a} \odot \exp\left(-\frac{\boldsymbol{u}^{*} + \zeta^{*}}{\tau_{a}}\right), \boldsymbol{\pi}^{T} \mathbf{1}_{M} = \boldsymbol{b},$$
 (6)

where u^* and ζ^* are the optimal value of u and ζ . The detailed proof is in Section A.3. That is, if we partially solve u and ζ , SemiUOT can be simplified to classical OT. Common exact solutions for u

and ζ are L-BFGS (Liu & Nocedal, 1989) or FISTA (Beck & Teboulle, 2009). The key insight is that solving the simplified classical OT for the OOD score using an exact OT solver is equivalent to obtaining it directly from the source weight in Equation (6).

Since the above approach is to obtain the equivalent form of SemiUOT via dynamically reweighting the weights of the source distribution, we name it **dynamic score aggregation** (DSA). By eschewing the entropy regularization responsible for unreliable scores and the arbitrary amplification of source weights, DSA achieves more accurate OOD detection without the computational burden of directly solving the full optimal transport plan. However, if we review the exact SemiUOT equation:

$$\min_{\mathbf{u},\zeta} \mathcal{J}_{S} = \tau_{a} \sum_{i=1}^{M} a_{i} \exp\left(-\frac{u_{i} + \zeta}{\tau_{a}}\right) - \sum_{j=1}^{N} \left[\inf_{k \in [M]} \left[C_{kj} - u_{k}\right] - \zeta\right] b_{j},\tag{7}$$

although \mathcal{J}_S is convex and has unique solutions, the presence of $\inf(\cdot)$ renders it a non-smooth function, leading to inefficient optimization. Thus, to further accelerate the optimization process, we turn to the approximate solution of DSA with the following proposition.

Proposition 3.2 (Accelerating DSA with approximation). We consider a smooth approximation to replace $\inf(\cdot)$ as $\inf_{k \in [M]} [C_{kj} - f_k] \approx -\epsilon \log[\sum_{k=1}^M e^{\frac{f_k - C_{kj}}{\epsilon}}]$. Note that $\epsilon > 0$ denotes the balanced hyperparameter among precision and smoothness of the function. Smaller ϵ (e.g., ϵ approaches to 0) could lead to more accurate while less smooth solutions. Then we can obtain the proposed Approximate SemiUOT Equation as $\widehat{\mathcal{J}}_{\mathbb{S}}$ by replacing $\inf(\cdot)$ with the smoothness term for \widehat{f} ,

$$\min_{\mathbf{u},\zeta} \widehat{\mathcal{J}}_{S} = \tau_{a} \exp\left(-\frac{\zeta}{\tau_{a}}\right) \sum_{i=1}^{M} a_{i} \exp\left(-\frac{u_{i}}{\tau_{a}}\right) + \sum_{j=1}^{N} \left[\epsilon \log\left[\sum_{k=1}^{M} \exp\left(\frac{u_{k} - C_{kj}}{\epsilon}\right)\right] + \zeta\right] b_{j}. (8)$$

Then, u_i can be iteratively updated as follows:

$$u_i^{(l+1)} = \frac{\tau_a \epsilon}{\tau_a + \epsilon} \log \left(a_i \exp\left(-\frac{\zeta}{\tau_a}\right) \right) - \frac{\tau_a \epsilon}{\tau_a + \epsilon} \log \left[\sum_{j=1}^N \left[\frac{\exp\left(-\frac{C_{ij}}{\epsilon}\right)}{\sum_{k=1}^M \exp\left(\frac{u_k^{(l)} - C_{kj}}{\epsilon}\right)} \right] b_j \right]$$

$$= \mathcal{T}(u_i^{(l)}).$$
(9)

Meanwhile, ζ *can be computed as,*

$$\zeta = \tau_a \left[\log \left(\sum_{i=1}^M a_i \exp\left(-\frac{u_i}{\tau_a} \right) \right) - \log \left(\sum_{j=1}^N b_j \right) \right]. \tag{10}$$

With this approximation method, we can solve DSA more efficiently. The proof is in Section A.4. As shown by the following proposition, the approximation error will become smaller with smaller ϵ .

Proposition 3.3 (Approximation error). We consider the analysis between optimal results of u^o and \hat{u}^o and thus we set $\zeta = 0$ in SemiUOT. Then we define $E_p(u) = \mathcal{J}_S$ and $K_p(\hat{u}) = \hat{\mathcal{J}}_S - \epsilon \log M$. Hence we have the following relationships: (1) $K_P(u^o) \leq E_P(u^o) \leq E_P(\hat{u}^o) \leq K_P(\hat{u}^o) + \epsilon \log M$, (2) $K_P(\hat{u}^o) \leq K_P(u^o) \leq E_P(u^o) \leq K_P(u^o) + \epsilon \log M$, and thus shows $|K_P(u^o) - K_P(\hat{u}^o)| \leq \epsilon \log M$. Moreover we have:

$$|E_P(u^o) - K_P(\hat{u}^o)| \le |E_P(u^o) - K_P(u^o)| + |K_P(u^o) - K_P(\hat{u}^o)| \le 2\epsilon \log M.$$
 (11)

Therefore we can observe that u and \hat{u}^o will get closer with smaller ϵ .

Algorithm 1 Dynamic Score Aggregation for OOD Detection

Input: Optimization objective \mathcal{J}_{S} . Output: Pseudo OOD score S'.

Initialize $t=0, u^0=(\frac{1}{M}, \frac{1}{M}, \cdots, \frac{1}{M})$ and $\zeta=0;$ for $t=0,1,2,\cdots,T$ do

Obtain the optimal solution on $u^{(t+1)}$ via Equation (9).

Optimize ζ by considering $\frac{\partial \mathcal{J}_S}{\partial \zeta} = 0$ via Equation (10).

end

270

271

272

273 274 275

276

277

278

279

280 281

282 283 284

285

287

289 290

291 292

293

295

296

297

298

299

300

301 302

303 304

306

307

308

310

311

312

313

314

315

316

317 318 319

320 321

322

323

Obtain the classical OT format $\widehat{\mathcal{J}}_{S}$ via Equation (6).

The pseudo OOD score **S** of the unlabeled samples is computed as $\mathbf{S} = \mathbf{a} \odot \exp\left(-\frac{u^* + \zeta^*}{\tau_*}\right)$.

The pseudo OOD score of the labeled samples is set as $\mathbf{1}_N$.

return $S' = S \oplus 1_N$.

The detailed computation process of the pseudo OOD scores based on approximation accelerated DSA is provided in Algorithm 1, whose time complexity is O(MN). It is worth highlighting that the DSA approach can directly obtain the OOD score from the source marginal distribution of \mathcal{J}_S . thus avoiding the solution of π . With the supervision of S', we train the OOD detection head h to distinguish the OOD samples from the ID ones.

3.4 MATRIX CONTRASTIVE REGULARIZATION

To improve the overall performance of SDM, we leverage the advantage of contrastive learning and propose the MCR module as an auxiliary task under the semi-supervised learning framework.

Given the feature embedding of the source domain sample from different strong augmented views, Z₁. and \mathbf{Z}_s^2 , their corresponding reconstructed feature embedding are denoted as $\mathcal{Z}_1, \mathcal{Z}_2 = \mathcal{G}(\mathbf{Z}_s^1), \mathcal{G}(\mathbf{Z}_s^2)$, where $\mathcal{Z}_1, \mathcal{Z}_2 \in \mathbb{R}^{M \times d}$ and \mathcal{G} is the self-supervised learning head. We introduce the matrix information theory (Zhang et al., 2023) into open-set SSL and leverage the alignment loss and uniformity loss to construct the regularization term, guiding the feature encoder f to learn more effective feature embedding and improve the performance of the other two branches,

$$\mathcal{L}_{\text{align}}(\mathcal{Z}_{1}, \mathcal{Z}_{2}) = -\operatorname{tr}\left(\frac{1}{B}\mathcal{Z}_{1}\mathbf{H}_{B}\mathcal{Z}_{2}^{\top}\right) + \gamma \cdot \operatorname{MCE}\left(\frac{1}{B}\mathcal{Z}_{1}\mathbf{H}_{B}\mathcal{Z}_{1}^{\top}, \frac{1}{B}\mathcal{Z}_{2}\mathbf{H}_{B}\mathcal{Z}_{2}^{\top}\right),$$

$$\mathcal{L}_{\text{uni}}(\mathcal{Z}_{1}, \mathcal{Z}_{2}) = \operatorname{MCE}\left(\frac{1}{d}\mathbf{I}_{d}, \frac{1}{B}\mathcal{Z}_{1}\mathbf{H}_{B}\mathcal{Z}_{2}^{\top}\right),$$
(12)

where $\mathbf{H}_B = \mathbf{I}_B - \frac{1}{B} \mathbf{1}_B \mathbf{1}_B^{\top}$. The computation of the MCE function is as follows:

$$MCE(\mathbf{P}, \mathbf{Q}) = tr(-\mathbf{P}\log\mathbf{Q} + \mathbf{Q}), \tag{13}$$

where P,Q are two positive semi-definite matrices. The alignment loss aims to bring the positive sample pairs closer in the feature domain, while the uniformity loss forces the representation to be evenly distributed in the feature space, avoiding the aggregation of features in certain areas or even NC. As shown in Equation (12), \mathcal{L}_{uni} tends to guide the centered sample covariance matrix close to the unit matrix in terms of expression. That is, if \mathcal{L}_{uni} is minimized as much as possible, different sample categories will be more evenly distributed in the feature space. Then, the contrastive regularization term is,

$$\mathcal{L}_{mcr} = \mathcal{L}_{align}(\mathcal{Z}_1, \mathcal{Z}_2) + \mathcal{L}_{uni}(\mathcal{Z}_1, \mathcal{Z}_2). \tag{14}$$

The detailed algorithm is presented in Section A.2. With both MCR and DSA, a novel open-set OOD detection framework SDM is constructed, which trains a neural OOD detector with the OOD scores produced by DSA as the supervision and boosts the overall performance via the MCR module.

EXPERIMENTS

4.1 SETUP

Datasets. We build open-set OOD benchmarks based on CIFAR-10 and CIFAR-100 (Krizhevsky et al., 2009) with different settings. By artificially dividing known classes as labeled samples, the

Table 1: Top-1 accuracy and AUROC on CIFAR-10 benchmarks under different settings. To verify the statistical significance of the results, we report both the mean and standard deviation of 5 experiments.

# of Labeled Classes	50		10	00	400		
Metric	Acc	AUROC	Acc	AUROC	Acc	AUROC	
MTCF	79.7±0.9	96.6±0.5	86.3±0.9	98.2±0.3	91.0 ± 0.5	98.9±0.1	
T2T	88.2 ± 0.7	75.5 ± 0.5	89.0 ± 1.0	77.2 ± 0.2	90.3 ± 0.5	82.3 ± 0.2	
OpenMatch	89.6 ± 0.9	99.3 ± 0.3	92.9 ± 0.5	99.7 ±0.2	94.1 ± 0.5	99.3 ± 0.2	
POT	92.1 ± 0.2	99.7 ±0.1	92.9 ± 0.2	99.5 ± 0.1	93.6 ± 0.1	99.4 ± 0.1	
SDM	92.5 ±0.4	99.6±0.2	93.1 ±0.1	99.5±0.2	94.2 ±0.1	99.4 ±0.3	

Table 2: Top-1 accuracy and AUROC on CIFAR-100 benchmarks under different settings. To verify the statistical significance of the results, we report both the mean and standard deviation of 5 experiments.

# of Known	55				80			
# of Labeled	5	0	100		50		100	
Metric	Acc	AUROC	Acc	AUROC	Acc	AUROC	Acc	AUROC
MTCF	66.5±1.2	81.2±3.4	72.1±0.5	80.7±4.6	59.9±0.8	79.4±2.5	66.4±0.3	73.2±3.5
T2T	$72.2 {\pm} 1.4$	$60.4 {\pm} 1.6$	$73.1{\pm}0.8$	$59.8 {\pm} 1.4$	$63.5 {\pm} 1.2$	$55.0 {\pm} 1.8$	$66.8 {\pm} 0.7$	55.4 ± 1.5
OpenMatch	$72.3 {\pm} 0.4$	87.0 ± 1.1	75.9 ± 0.6	$86.5{\pm}2.1$	66.6 ± 0.2	86.2 ± 0.6	$70.5 {\pm} 0.3$	$86.8 {\pm} 1.4$
POT	$78.7 {\pm} 0.1$	$88.4 {\pm} 0.1$	81.1 ± 0.1	$89.5 {\pm} 0.3$	75.4 ± 0.1	88.1 ± 0.3	78.1 ± 0.1	88.0 ± 0.1
SDM	$\textbf{78.9} \!\pm 0.3$	91.7 ±0.3	81.3 ±0.4	91.3 ±0.3	75.7 ±0.2	90.9 ±0.3	78.3 ±0.5	90.9 ±0.3

models need to detect OOD samples exist in X_u . Following the setup in (Sohn et al., 2020) and (Ren et al., 2024), the complete training set is used as unlabeled data, while labeled data is randomly extracted from the training set and the number of samples for each known class is set to different values corresponding to different classification difficulties. We also evaluate SDM on the more challenging ImageNet-30 (Hendrycks & Gimpel, 2017) dataset, where 20 classes are selected as the known classes, with the remaining as the unknown classes.

Baselines. To demonstrate the superiority of our method on OOD detection benchmark, we compare our proposed SDM with comprehensive baselines, including Fixmatch(Sohn et al., 2020), MTCF(Yu et al., 2020a), T2T(Huang et al., 2021a), OpenMatch(Saito et al., 2021), and POT(Ren et al., 2024). Since the semi-supervised classification module of SDM in this paper adopts the Fixmatch structure, we consider it as a baseline. The maximum softmax prediction probability as the score function is used to give Fixmatch the ability to perform OOD detection during testing. MTCF and T2T are typical purely neural networks based methods. OpenMatch adopts a method based on OVA classifiers. In addition, to prove the effectiveness of DSA, we also compare SDM with other OT-based method.

Metrics. To measure the OOD detection results, we calculate the area under the receiver operating characteristic curve (AUROC) to observe the ability to identify OOD samples. In this paper, we focus on image classification tasks in the presence of OOD samples, so we also report closed-set classification accuracy. In scenarios where we focus on comparing the performance of different methods, we report top-1 accuracy and AUROC, and in scenarios where we focus on analyzing the change with different architectures or parameter settings, we report top-1 to top-5 accuracy to facilitate comprehensive analysis. More settings and implementation details are provided in Section A.5.

4.2 RESULTS AND DISCUSSION

The experimental results on CIFAR-10, CIFAR-100, and ImageNet-30 are summarized in Table 1, Table 2, and Table 3. Our analysis reveals a clear performance hierarchy. Methods relying solely on neural networks perform poorly across all datasets, lagging significantly behind proxy-based approaches. While OpenMatch shows competitive results on CIFAR-10, it falls short of OT-based methods, particularly on CIFAR-100 where its closed-set accuracy is lower. Overall, SDM achieves

Table 3: Top-1 accuracy and AUROC on ImageNet-30 benchmarks. 20 classes are selected as known classes, and the remaining classes are unknown classes.

Method	FixMatch	MTCF	T2T	OpenMatch	POT	Ours
Top1Acc	91.7±0.5	86.4 ± 0.7	87.8 ± 0.9	89.6 ± 1.0	92.0 ± 0.3	92.1 ±0.4
AUROC	45.1 ± 1.2	$93.8 {\pm} 0.8$	55.7 ± 10.8	96.4 ± 0.7	97.4 ± 0.4	97.7 ±0.2

Table 4: Ablation study on CIFAR-10 benchmark. Fixmatch-OOD use the maximum softmax prediction probability to give Fixmatch the ability to perform OOD detection during training phase.

# of Labeled Classes	50		10	00	400		
Metric	Acc	AUROC	Acc	AUROC	Acc	AUROC	
FixMatch-OOD	91.7±1.1	37.7±0.6	92.9±0.7	39.8±0.3	93.4±0.3	40.9±0.6	
Fixmatch+DSA	92.2 ± 0.3	99.6 ± 0.1	93.0 ± 0.3	99.5 ± 0.2	94.1 ± 0.2	99.4 ± 0.1	
Fixmatch+DSA+MCR	92.5 ±0.4	99.6 ±0.2	93.1 ±0.1	99.5 ±0.2	94.2 ±0.1	99.4 ±0.3	

better performance than POT and maintains competitive performance on the more challenging ImageNet-30 dataset with 224×224 resolution. The most significant advantage of SDM is observed in AUROC on CIFAR-100, a gain potentially attributable to the larger number of classes, which causes other methods to not be able to perform OOD detection well.

Table 5: Adaptation to different OT solvers. We report top-1 to top-5 accuracy and AUROC on CIFAR-100 with 55 known classes and 50 labeled samples per known class, with POT as the baseline.

Metirc	Solver	Type	Solution			Acc			AUROC
		31		Top1	Top2	Top3	Top4	Top5	
POT	POT	Partial OT	Approximate	78.4	87.7	91.5	93.8	95.0	90.1
DSA(+EPW)	EPW	OT	Approximate	79.0	88.1	91.8	93.7	95.0	91.0
DSA(+Sinkhorn)	Sinkhorn	OT	Approximate	79.2	88.0	91.9	93.8	95.3	91.2
DSA(+EMD)	EMD	OT	Exact	79.5	88.0	91.8	93.7	95.2	91.5

4.3 Adaptation to different OT solvers

Since DSA dynamically converts the SemiUOT from α to β in each batch into classical OT during training, in theory any classical OT solver can be connected in series behind DSA. In order to verify the adaptability of SDM to different OT solvers, we insert several OT solvers into SDM for trial, including EMD, Sinkhorn and entropic partial wasserstein (EPW) (Cuturi, 2013). Besides, we also report the results of POT as a baseline in Table 5. The SDM plugged into three different OT solvers all outperformed POT in terms of metrics. Interestingly, when we directly connect modules similar to those in POT in series to DSA, we can also observe performance improvements. Since EMD obtains an exact solution, while others obtain approximate solutions, the OOD labels obtained based on DSA and EMD are more reliable.

4.4 Analysis and ablation study

1) Ablation study. Table 4 reports the overall performance of Fixmath-OOD, Fixmatch+DSA and Fixmatch+DSA+MCR. Fixmatch itself cannot detect OOD samples accurately enough, even when performing OOD detection based on predicted probabilities during inference. When training OOD detector under the supervision of DSA, the AUROC metric which indicates the open-ser OOD detection quality reach an impressively higher lever compared to Fixmatch-OOD. With the support of MCR module as auxiliary task, we observe the improvement of the top-1 closed-set classification accuracy without the sacrifice of AUROC. Performance improvement of the DSA method and the MCR module does not come at the cost of testing latency because only Fixmatch and neural networks

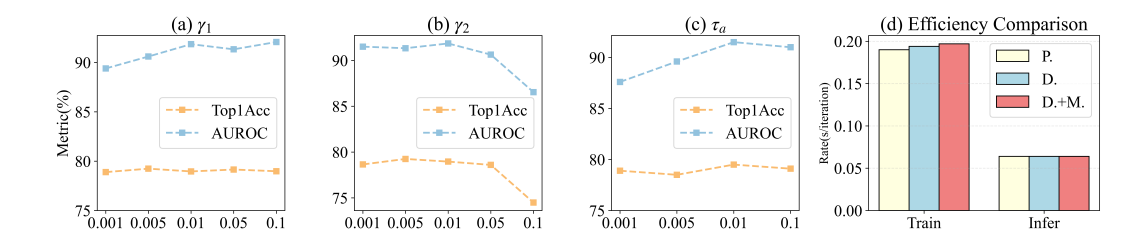


Figure 2: (a) The change of performance with γ_1 when γ_2 is fixed to 0.01. (b) The change of performance with γ_2 when γ_1 is fixed to 0.01. (c) The change of performance with τ_a . (d) The efficiency comparison of P.(POT), D.(DSA), and D.+M.(DSA+MCR). All results are on CIFAR-100 benchmark with 55 known classes and 50 labeled samples per known class.

that output ID probability are activated during the training phase. With MCR, we can observe an improvement in closed-set accuracy or OOD detection quality without sacrificing the other metric.

2) Quantitative analysis of the pseudo labels. In Table 6, We compare the AUROC of the pseudo lables produced by DSA to that of POT with the additional parameter set to 1.25 and 2.5 respectively. All the experiments are conducted on test datasets with labeled training samples as the target samples. The pseudo labels produced by DSA are more accurate than POT.

Table 6: Quantitative analysis of the accuracy of the pseudo labels on CIFAR-100.

# of Known	5	5	80		
# of Labeled	50	100	50	100	
POT(k = 1.25)	54.9	54.9	58.0	55.2	
POT(k = 2.5)	59.2	58.7	60.0	57.9	
DSA	59.7	59.2	60.1	58.3	

3) Influence of \mathcal{L}_{ood} and \mathcal{L}_{mcr} . Since SDM is a multi-task learning framework, the coefficients of the loss functions corresponding to different tasks are

important. Figure 2 (a) and (b) depict the changes of top-1 classification accuracy and OOD detection quality with γ_1 and γ_2 corresponding to \mathcal{L}_{ood} and \mathcal{L}_{mcr} respectively. Besides, when the value of γ_1 is too small, such as 0.01, the impact of \mathcal{L}_{ood} on the overall loss is too small to make the quality of OOD detection worse. In other cases, SDM is stable enough to the changes of relevant core parameters.

- 4) Influence of τ_a . As we can see that, the larger value of τ_a in Equation (2) involves more data to get matched. Figure 2 (c) reports the results with τ_a changes to check the influence of this property on SDM. Given that τ_a is essentially a scaling factor, our experiments span a fairly large range from 0.001 to 1, where no significant increase or decrease in performance is observed. Thus τ_a does not need to be overly fine-tuned to adapt to specific tasks and shows sufficient robustness.
- 5) Efficiency Analysis. To validate that the improvement of performance does not come at the cost of significant delay, we count the execution rate of SDM and its variants (i.e., FixMatch+DSA) compared with the baseline. The training rate and testing rate are calculated as the average rate within 1024 iterations in Figure 2 (d). Owing to the acceleration approach of Proposition 3.2, the training latency of DSA is modest compared to POT. The additional computational cost of MCR is also acceptable. Consistent with the analysis in this paper, both DSA and MCR cause no test delay. In addition, the training rate of SDM is 1.25s/iteration on the ImageNet-30 dataset, which means only 6.3×1 latency at 49×1 resolution compared to the case on CIFAR-10/100.

5 CONCLUSION

In summary, we propose a novel open-set semi-supervised OOD detection framework SDM, which synergistically leverages the advantages of SSL, self-supervised learning, and OT. Through theoretical derivation, we innovatively propose the accelerated DSA method that dynamically converts SemiUOT into classical OT and provides reliable pseudo OOD lables for supervision. Using the MCR module as an auxiliary task for semi-supervised classification and OOD detection, SDM comprehensively surpasses all baselines on all benchmarks, especially dominating the open-set OOD detection benchmarks based on CIFAR-100. Our proposal will further motivate future work to pursue more novel and efficient learning paradigms or frameworks for open-set SSL.

REFERENCES

- Arip Asadulaev, Rostislav Korst, Alexander Korotin, Vage Egiazarian, Andrey Filchenkov, and Evgeny Burnaev. Rethinking optimal transport in offline reinforcement learning. *arXiv* preprint arXiv:2410.14069, 2024.
- Amir Beck and Marc Teboulle. A fast iterative shrinkage-thresholding algorithm for linear inverse problems. *SIAM journal on imaging sciences*, 2(1):183–202, 2009.
- David Berthelot, Nicholas Carlini, Ian Goodfellow, Nicolas Papernot, Avital Oliver, and Colin A Raffel. Mixmatch: A holistic approach to semi-supervised learning. *Advances in neural information processing systems*, 32, 2019.
- Changrui Chen, Jungong Han, and Kurt Debattista. Virtual category learning: A semi-supervised learning method for dense prediction with extremely limited labels. *IEEE transactions on pattern analysis and machine intelligence*, 2024.
- Xuxin Cheng, Zhihong Zhu, Hongxiang Li, Yaowei Li, Xianwei Zhuang, and Yuexian Zou. Towards multi-intent spoken language understanding via hierarchical attention and optimal transport. In *Proceedings of the AAAI Conference on Artificial Intelligence*, volume 38, pp. 17844–17852, 2024a.
- Xuxin Cheng, Zhihong Zhu, Hongxiang Li, Yaowei Li, Xianwei Zhuang, and Yuexian Zou. Towards multi-intent spoken language understanding via hierarchical attention and optimal transport. In *Proceedings of the AAAI Conference on Artificial Intelligence*, volume 38, pp. 17844–17852, 2024b.
- Jaemoo Choi, Jaewoong Choi, and Myungjoo Kang. Generative modeling through the semi-dual formulation of unbalanced optimal transport. *Advances in Neural Information Processing Systems*, 36:42433–42455, 2023.
- Sayeed Shafayet Chowdhury, Soumyadeep Chandra, and Kaushik Roy. Opel: Optimal transport guided procedure learning. In *The Thirty-eighth Annual Conference on Neural Information Processing Systems*.
- Marco Cuturi. Sinkhorn distances: Lightspeed computation of optimal transport. *Advances in neural information processing systems*, 26, 2013.
- Jean-Bastien Grill, Florian Strub, Florent Altché, Corentin Tallec, Pierre Richemond, Elena Buchatskaya, Carl Doersch, Bernardo Avila Pires, Zhaohan Guo, Mohammad Gheshlaghi Azar, et al. Bootstrap your own latent-a new approach to self-supervised learning. *Advances in neural information processing systems*, 33:21271–21284, 2020.
- Lan-Zhe Guo, Zhen-Yu Zhang, Yuan Jiang, Yu-Feng Li, and Zhi-Hua Zhou. Safe deep semi-supervised learning for unseen-class unlabeled data. In *International conference on machine learning*, pp. 3897–3906. PMLR, 2020.
- Kaiming He, Xiangyu Zhang, Shaoqing Ren, and Jian Sun. Deep residual learning for image recognition. In *Proceedings of the IEEE conference on computer vision and pattern recognition*, pp. 770–778, 2016.
- Rundong He, Zhongyi Han, Xiankai Lu, and Yilong Yin. Safe-student for safe deep semi-supervised learning with unseen-class unlabeled data. In *Proceedings of the IEEE/CVF conference on computer vision and pattern recognition*, pp. 14585–14594, 2022.
- Dan Hendrycks and Kevin Gimpel. A baseline for detecting misclassified and out-of-distribution examples in neural networks. *arXiv preprint arXiv:1610.02136*, 2016.
- Dan Hendrycks and Kevin Gimpel. A baseline for detecting misclassified and out-of-distribution examples in neural networks. In *International Conference on Learning Representations*, 2017.
- Junkai Huang, Chaowei Fang, Weikai Chen, Zhenhua Chai, Xiaolin Wei, Pengxu Wei, Liang Lin, and Guanbin Li. Trash to treasure: Harvesting ood data with cross-modal matching for open-set semi-supervised learning. In *Proceedings of the IEEE/CVF international conference on computer vision*, pp. 8310–8319, 2021a.

- Rui Huang, Andrew Geng, and Yixuan Li. On the importance of gradients for detecting distributional shifts in the wild. *Advances in Neural Information Processing Systems*, 34:677–689, 2021b.
 - Ka-Hei Hui, Chao Liu, Xiaohui Zeng, Chi-Wing Fu, and Arash Vahdat. Not-so-optimal transport flows for 3d point cloud generation. *arXiv preprint arXiv:2502.12456*, 2025.
 - Sontje Ihler, Felix Kuhnke, Timo Kuhlgatz, and Thomas Seel. Distribution-aware multi-label fixmatch for semi-supervised learning on chexpert. In *Proceedings of the IEEE/CVF Conference on Computer Vision and Pattern Recognition*, pp. 2295–2304, 2024.
 - Sergio Izquierdo and Javier Civera. Optimal transport aggregation for visual place recognition. In *Proceedings of the ieee/cvf conference on computer vision and pattern recognition*, pp. 17658–17668, 2024.
 - Prakhar Kaushik, Adam Kortylewski, and Alan Yuille. A bayesian approach to ood robustness in image classification. In *Proceedings of the IEEE/CVF Conference on Computer Vision and Pattern Recognition*, pp. 22988–22997, 2024.
 - Abdelwahed Khamis, Russell Tsuchida, Mohamed Tarek, Vivien Rolland, and Lars Petersson. Scalable optimal transport methods in machine learning: A contemporary survey. *IEEE Transactions on Pattern Analysis and Machine Intelligence*, pp. 1–20, 2024. doi: 10.1109/TPAMI.2024.3379571.
 - Durk P Kingma, Shakir Mohamed, Danilo Jimenez Rezende, and Max Welling. Semi-supervised learning with deep generative models. *Advances in neural information processing systems*, 27, 2014.
 - Pascal Klink, Carlo D'Eramo, Jan Peters, and Joni Pajarinen. On the benefit of optimal transport for curriculum reinforcement learning. *IEEE Transactions on Pattern Analysis and Machine Intelligence*, 2024.
 - Alex Krizhevsky, Geoffrey Hinton, et al. Learning multiple layers of features from tiny images.(2009), 2009.
 - Khang Le, Huy Nguyen, Quang M Nguyen, Tung Pham, Hung Bui, and Nhat Ho. On robust optimal transport: Computational complexity and barycenter computation. *Advances in Neural Information Processing Systems*, 34:21947–21959, 2021.
 - Doyup Lee, Sungwoong Kim, Ildoo Kim, Yeongjae Cheon, Minsu Cho, and Wook-Shin Han. Contrastive regularization for semi-supervised learning. In *Proceedings of the IEEE/CVF conference on computer vision and pattern recognition*, pp. 3911–3920, 2022.
 - Gang Li, Xiang Li, Yujie Wang, Yichao Wu, Ding Liang, and Shanshan Zhang. Pseco: Pseudo labeling and consistency training for semi-supervised object detection. In *European Conference on Computer Vision*, pp. 457–472. Springer, 2022a.
 - Hengduo Li, Zuxuan Wu, Abhinav Shrivastava, and Larry S Davis. Rethinking pseudo labels for semi-supervised object detection. In *Proceedings of the AAAI conference on artificial intelligence*, volume 36, pp. 1314–1322, 2022b.
 - Junnan Li, Caiming Xiong, and Steven CH Hoi. Comatch: Semi-supervised learning with contrastive graph regularization. In *Proceedings of the IEEE/CVF international conference on computer vision*, pp. 9475–9484, 2021.
 - Qian Li, Zhichao Wang, Haiyang Xia, Gang Li, Yanan Cao, Lina Yao, and Guandong Xu. Hotgan: Hilbert optimal transport for generative adversarial network. *IEEE Transactions on Neural Networks and Learning Systems*, 2024.
 - Rui Li, Tingting Ren, Jie Wen, and Jinxing Li. Optimal transport-based labor-free text prompt modeling for sketch re-identification. *Advances in Neural Information Processing Systems*, 37: 119198–119226, 2025.
 - Zekun Li, Lei Qi, Yinghuan Shi, and Yang Gao. Iomatch: Simplifying open-set semi-supervised learning with joint inliers and outliers utilization. In *Proceedings of the IEEE/CVF International Conference on Computer Vision*, pp. 15870–15879, 2023.

- Wei Lin and Antoni B Chan. Optimal transport minimization: Crowd localization on density maps for semi-supervised counting. In *Proceedings of the IEEE/CVF Conference on Computer Vision and Pattern Recognition*, pp. 21663–21673, 2023.
- Dong C Liu and Jorge Nocedal. On the limited memory bfgs method for large scale optimization. *Mathematical programming*, 45(1):503–528, 1989.
- Weitang Liu, Xiaoyun Wang, John Owens, and Yixuan Li. Energy-based out-of-distribution detection. *Advances in neural information processing systems*, 33:21464–21475, 2020.
- Yiwei Lu, Guojun Zhang, Sun Sun, Hongyu Guo, and Yaoliang Yu. f-micl: Understanding and generalizing infonce-based contrastive learning. arXiv preprint arXiv:2402.10150, 2024.
- Qiankun Ma, Jiyao Gao, Bo Zhan, Yunpeng Guo, Jiliu Zhou, and Yan Wang. Rethinking safe semi-supervised learning: Transferring the open-set problem to a close-set one. In *Proceedings of the IEEE/CVF International Conference on Computer Vision*, pp. 16370–16379, 2023.
- Hermina Petric Maretic, Mireille El Gheche, Giovanni Chierchia, and Pascal Frossard. Fgot: Graph distances based on filters and optimal transport. In *Proceedings of the AAAI Conference on Artificial Intelligence*, volume 36, pp. 7710–7718, 2022.
- Zeping Min, Jinfeng Bai, and Chengfei Li. Leveraging local variance for pseudo-label selection in semi-supervised learning. In *Proceedings of the AAAI Conference on Artificial Intelligence*, volume 38, pp. 14370–14378, 2024.
- Yuehan Qin, Yichi Zhang, Yi Nian, Xueying Ding, and Yue Zhao. Metaood: Automatic selection of ood detection models. *arXiv preprint arXiv:2410.03074*, 2024.
- Yilong Ren, Chuanwen Feng, Xike Xie, and S Kevin Zhou. Partial optimal transport based out-of-distribution detection for open-set semi-supervised learning. In *Proceedings of the Thirty-Third International Joint Conference on Artificial Intelligence*, pp. 4851–4859, 2024.
- Kuniaki Saito, Donghyun Kim, and Kate Saenko. Openmatch: Open-set consistency regularization for semi-supervised learning with outliers. *arXiv preprint arXiv:2105.14148*, 2021.
- Xu Shen, Yili Wang, Kaixiong Zhou, Shirui Pan, and Xin Wang. Optimizing ood detection in molecular graphs: A novel approach with diffusion models. In *Proceedings of the 30th ACM SIGKDD Conference on Knowledge Discovery and Data Mining*, pp. 2640–2650, 2024.
- Kihyuk Sohn, David Berthelot, Nicholas Carlini, Zizhao Zhang, Han Zhang, Colin A Raffel, Ekin Dogus Cubuk, Alexey Kurakin, and Chun-Liang Li. Fixmatch: Simplifying semi-supervised learning with consistency and confidence. *Advances in neural information processing systems*, 33:596–608, 2020.
- Tiberiu Sosea and Cornelia Caragea. Marginmatch: Improving semi-supervised learning with pseudomargins. In *Proceedings of the IEEE/CVF conference on computer vision and pattern recognition*, pp. 15773–15782, 2023.
- Mingyang Sun, Pengxiang Ding, Weinan Zhang, and Donglin Wang. Score-based diffusion policy compatible with reinforcement learning via optimal transport. *arXiv preprint arXiv:2502.12631*, 2025.
- Ziteng Sun, Ananda Theertha Suresh, Jae Hun Ro, Ahmad Beirami, Himanshu Jain, and Felix Yu. Spectr: Fast speculative decoding via optimal transport. Advances in Neural Information Processing Systems, 36:30222–30242, 2023.
- Alexander Tong, Kilian Fatras, Nikolay Malkin, Guillaume Huguet, Yanlei Zhang, Jarrid Rector-Brooks, Guy Wolf, and Yoshua Bengio. Improving and generalizing flow-based generative models with minibatch optimal transport. *arXiv preprint arXiv:2302.00482*, 2023a.
- Alexander Tong, Nikolay Malkin, Guillaume Huguet, Yanlei Zhang, Jarrid Rector-Brooks, Kilian Fatras, Guy Wolf, and Yoshua Bengio. Conditional flow matching: Simulation-free dynamic optimal transport. *arXiv preprint arXiv:2302.00482*, 2(3), 2023b.

- Ruixuan Xiao, Lei Feng, Kai Tang, Junbo Zhao, Yixuan Li, Gang Chen, and Haobo Wang. Targeted representation alignment for open-world semi-supervised learning. In *Proceedings of the IEEE/CVF Conference on Computer Vision and Pattern Recognition*, pp. 23072–23082, 2024.
- Yang Yang, Nan Jiang, Yi Xu, and De-Chuan Zhan. Robust semi-supervised learning by wisely leveraging open-set data. *IEEE Transactions on Pattern Analysis and Machine Intelligence*, 2024.
- Qing Yu, Daiki Ikami, Go Irie, and Kiyoharu Aizawa. Multi-task curriculum framework for open-set semi-supervised learning. In *Computer Vision–ECCV 2020: 16th European Conference, Glasgow, UK, August 23–28, 2020, Proceedings, Part XII 16*, pp. 438–454. Springer, 2020a.
- Qing Yu, Daiki Ikami, Go Irie, and Kiyoharu Aizawa. Multi-task curriculum framework for open-set semi-supervised learning. In *Computer Vision–ECCV 2020: 16th European Conference, Glasgow, UK, August 23–28, 2020, Proceedings, Part XII 16*, pp. 438–454. Springer, 2020b.
- Sergey Zagoruyko and Nikos Komodakis. Wide residual networks. arXiv preprint arXiv:1605.07146, 2016.
- Jure Zbontar, Li Jing, Ishan Misra, Yann LeCun, and Stéphane Deny. Barlow twins: Self-supervised learning via redundancy reduction. In *International conference on machine learning*, pp. 12310–12320. PMLR, 2021.
- Zhichen Zeng, Si Zhang, Yinglong Xia, and Hanghang Tong. Parrot: Position-aware regularized optimal transport for network alignment. In *Proceedings of the ACM Web Conference* 2023, pp. 372–382, 2023.
- Zhichen Zeng, Boxin Du, Si Zhang, Yinglong Xia, Zhining Liu, and Hanghang Tong. Hierarchical multi-marginal optimal transport for network alignment. In *Proceedings of the AAAI Conference on Artificial Intelligence*, volume 38, pp. 16660–16668, 2024.
- Xiaohua Zhai, Avital Oliver, Alexander Kolesnikov, and Lucas Beyer. S4l: Self-supervised semi-supervised learning. In *Proceedings of the IEEE/CVF international conference on computer vision*, pp. 1476–1485, 2019.
- Yifan Zhang, Zhiquan Tan, Jingqin Yang, Weiran Huang, and Yang Yuan. Matrix information theory for self-supervised learning. *arXiv preprint arXiv:2305.17326*, 2023.
- Yifei Zhang, Hao Zhu, Zixing Song, Yankai Chen, Xinyu Fu, Ziqiao Meng, Piotr Koniusz, and Irwin King. Geometric view of soft decorrelation in self-supervised learning. In *Proceedings of the 30th ACM SIGKDD Conference on Knowledge Discovery and Data Mining*, pp. 4338–4349, 2024.
- Mingkai Zheng, Shan You, Lang Huang, Fei Wang, Chen Qian, and Chang Xu. Simmatch: Semi-supervised learning with similarity matching. In *Proceedings of the IEEE/CVF conference on computer vision and pattern recognition*, pp. 14471–14481, 2022.

APPENDIX

702

703 704

705 706

708

709

710

711

712

713

714

715

716

717

718

719

720

721

722

723

724

725

726

727

728 729 730

731 732 733

734

735

736

737 738 739

740

742 743 744

745 746

747 748

749

750 751

752

753

754

755

ALGORITHM OF SDM

Algorithm 2 Open-Set Out-of-Distribution Detection

Require: Data loader, weak augmentation method A, strong augmentation method A, encoder network $f(\cdot)$, closed-set classification head $g(\cdot)$, OOD detection head $h(\cdot)$ and SSL head $\mathcal{G}(\cdot)$.

for X_l, X_u in loader do

```
Augmentation:
```

$$\mathbf{X}_w, \mathbf{X}_s^1, \mathbf{X}_s^2 = A(\mathbf{X}_u), \mathcal{A}(\mathbf{X}_u), \mathcal{A}(\mathbf{X}_u).$$

Encoding:

$$\mathbf{Z}_l, \mathbf{Z}_w, \mathbf{Z}_s^1, \mathbf{Z}_s^2 = f(\mathbf{X}_l), f(\mathbf{X}_w), f(\mathbf{X}_s^1), f(\mathbf{X}_s^2).$$

OOD detection:

Compute the cosine similarity C between \mathbf{Z}_l and \mathbf{Z}_s^1 .

Obtain OOD pseudo labels S' via the DSA approach.

Obtain OOD predicted score $\hat{\mathbf{S}} = h(\mathbf{Z}_l, \mathbf{Z}_s^1)$.

Compute OOD loss \mathcal{L}_{ood} .

MCR:

Obtain \mathcal{L}_{mcr} via Algorithm 3.

Self-supervised classification:

Obatin classification probability

$$\mathcal{Y}_l, \mathcal{Y}_w, \mathcal{Y}_s^1 = g(\mathbf{Z}_l), g(\mathbf{Z}_w), g(\mathbf{Z}_s^1).$$

Compute supervised loss \mathcal{L}_x and unspervised loss \mathcal{L}_u .

Total loss:

$$\mathcal{L} = \mathcal{L}_x + \mathcal{L}_u + \gamma_1 \mathcal{L}_{ood} + \gamma_2 \mathcal{L}_{mcr}.$$

Back propagation.

end

A.2 ALGORITHM OF MCR

Algorithm 3 Matrix Contrastive Regularization

Input: Batch of unlabeled sample X_u , strong augmentation method A, encoder network $f(\cdot)$ and contrastive learning head $\mathcal{G}(\cdot)$.

Output: MCR loss.

Augmentation: $\mathbf{X}_s^1, \mathbf{X}_s^1 = \mathcal{A}(\mathbf{X}_u), \mathcal{A}(\mathbf{X}_u).$ Encoding: $\mathbf{Z}_s^1, \mathbf{Z}_s^2 = f(\mathbf{X}_s^1), f(\mathbf{X}_s^2).$ Projecting and predicting: $\mathcal{Z}_s^1, \mathcal{Z}_s^2 = \mathcal{G}(\mathbf{Z}_s^1), \mathcal{G}(\mathbf{Z}_s^2).$

Obtain $\mathcal{L}_{\text{Matrix-Alignment}}$ and $\mathcal{L}_{\text{Matrix-Uniformity}}$ via Equation (12).

MCR loss: $\mathcal{L}_{mcr} = \mathcal{L}_{\text{Matrix-Alignment}} + \mathcal{L}_{\text{Matrix-Uniformity}}$. 741

Return \mathcal{L}_{mcr} .

A.3 Proof of Proposition 3.1

We can rewrite the SemiUOT problem as below:

$$\begin{split} & \min_{\boldsymbol{\pi} \geq 0} J = \langle \boldsymbol{C}, \boldsymbol{\pi} \rangle + \tau_a \mathrm{KL}\left(\boldsymbol{\pi} \mathbf{1}_N \| \boldsymbol{a}\right) \\ & s.t. \text{ (Constraint)}: \boldsymbol{\pi}^\top \mathbf{1}_M = \boldsymbol{b}, \text{(Optional)}: \boldsymbol{\pi} \mathbf{1}_N = \boldsymbol{\alpha}. \end{split}$$

Note that we do not need to know the exact value of α beforehand. We adopt this optional constraint only for simplifying the following deduction. The Lagrange multipliers of Semi-UOT with KL-Divergence is given as:

$$\max_{\boldsymbol{s} \geq 0, \boldsymbol{u}, \boldsymbol{v}, \zeta} \min_{\boldsymbol{\pi} \geq 0} \mathcal{J} = \tau_a \text{KL} \left(\boldsymbol{\pi} \mathbf{1}_N \| \boldsymbol{a} \right) + \langle \boldsymbol{u} + \zeta, \boldsymbol{\pi} \mathbf{1}_N \rangle + \langle \boldsymbol{v} - \zeta, \boldsymbol{b} \rangle + \mathscr{C}_{\text{SUOT}},$$

where $\mathscr{C}_{SUOT} = \sum_{i,j} (C_{ij} - u_i - v_j - s_{ij}) \pi_{ij} = \langle \boldsymbol{C} - \boldsymbol{u} \otimes \boldsymbol{1}_N^\top - \boldsymbol{1}_M \otimes \boldsymbol{v}^\top - \boldsymbol{s}, \boldsymbol{\pi} \rangle$ and $\boldsymbol{u}, \boldsymbol{v}$ and ζ are dual variables. By taking the differentiation on π_{ij} we have:

$$\frac{\partial \mathcal{J}}{\partial \pi_{ij}} = \left[\tau_a \log \frac{\sum_{j=1}^N \pi_{ij}}{a_i} + u_i + \zeta \right] + (C_{ij} - u_i - v_j - s_{ij})$$
$$= C_{ij} + \tau_a \log \frac{\sum_{j=1}^N \pi_{ij}}{a_i} + \zeta - v_j - s_{ij} = 0.$$

Then we can obtain the results:

$$\begin{cases} \sum_{j=1}^{N} \pi_{ij} = a_i \exp\left(-\frac{u_i + \zeta}{\tau_a}\right) \\ \sum_{i=1}^{M} \pi_{ij} = b_j \end{cases} \Rightarrow C_{ij} - u_i - v_j - s_{ij} = 0, \quad s_{ij} \ge 0.$$

Thus SemiUOT can be can be regarded as classic optimal transport problem:

$$egin{aligned} \min_{m{\pi} \geq 0} \mathcal{J}_{\mathrm{S}} &= \langle m{C}, m{\pi}
angle \\ s.t. m{\pi} \mathbf{1}_N &= m{a} \odot \exp\left(-rac{m{u}^* + \zeta^*}{ au_a}
ight), m{\pi}^ op \mathbf{1}_M = m{b}. \end{aligned}$$

A.4 PROOF OF PROPOSITION 3.2

We first review the Exact SemiUOT Equation:

$$\min_{\mathbf{u},\zeta} \mathcal{J}_{S} = \tau_{a} \sum_{i=1}^{M} a_{i} \exp\left(-\frac{u_{i} + \zeta}{\tau_{a}}\right) - \sum_{i=1}^{N} \left[\inf_{k \in [M]} \left[C_{kj} - u_{k}\right] - \zeta\right] b_{j}.$$

Then we take the differentiation on u_i to obtain:

$$\left\| \frac{\partial \mathcal{J}_{S}}{\partial u_{i}} \right\| = \left\| -a_{i} \exp\left(-\frac{u_{i} + \zeta}{\tau_{a}}\right) + \sum_{j=1}^{N} \delta\left(i = \arg\min_{k \in [M]} \left[C_{kj} - u_{k}\right]\right) b_{j} \right\|$$

$$\leq \left\| a_{i} \exp\left(-\frac{u_{i} + \zeta}{\tau_{a}}\right) \right\| + \left\| \sum_{j=1}^{N} \delta\left(i = \arg\min_{k \in [M]} \left[C_{kj} - u_{k}\right]\right) b_{j} \right\|$$

$$\leq \left\| \sum_{j=1}^{N} b_{j} \right\| + \left\| \sum_{j=1}^{N} b_{j} \right\|$$

$$= 2 \sum_{j=1}^{N} b_{j} = \mathcal{L}.$$

Therefore, it satisfies the Lipchitz constraints in gradient descend

$$||\mathcal{J}_{\mathrm{S}}(\boldsymbol{u}_y) - \mathcal{J}_{\mathrm{S}}(\boldsymbol{u}_x)|| \leq \mathcal{L}||\boldsymbol{u}_y - \boldsymbol{u}_x||.$$

Finally we can adopt SGD with step-size as $\eta = \frac{1}{\mathscr{L}}$ for the optimization:

$$u_i^{(\text{new})} = u_i^{(\text{old})} - \frac{1}{\mathscr{L}} \left[\sum_{j=1}^N \delta \left(i = \arg\min_{k \in [M]} \left[C_{kj} - u_k^{(\text{old})} \right] \right) b_j - a_i \exp\left(-\frac{u_i^{(\text{old})} + \zeta}{\tau_a} \right) \right].$$

Although \mathcal{J}_S is convex and has unique solutions, the presence of $\inf(\cdot)$ renders it a non-smooth function, leading to inefficient optimization. To further accelerate the optimization process, we consider to make a smooth approximation on replacing $\inf(\cdot)$ as $\inf_{k\in[M]}[C_{kj}-f_k]\approx -\epsilon\log[\sum_{k=1}^M e^{\frac{f_k-C_{kj}}{\epsilon}}]$. Note that $\epsilon>0$ denotes the balanced hyper parameters among the accuracy and function smoothness. Smaller ϵ (e.g., ϵ approaches to 0) could lead to more accurate while less smooth solutions. Then

we can obtain the proposed *Approximate SemiUOT Equation* as $\widehat{\mathcal{J}}_{\mathcal{S}}$ by replacing $\inf(\cdot)$ with the smoothness term for \widehat{f} as below:

$$\min_{\mathbf{u},\zeta} \widehat{\mathcal{J}}_{S} = \tau_{a} \exp\left(-\frac{\zeta}{\tau_{a}}\right) \sum_{i=1}^{M} a_{i} \exp\left(-\frac{u_{i}}{\tau_{a}}\right) + \sum_{j=1}^{N} \left[\epsilon \log\left[\sum_{k=1}^{M} \exp\left(\frac{u_{k} - C_{kj}}{\epsilon}\right)\right] + \zeta\right] b_{j}.$$

Take the differentiation on u_i we can obtain:

$$\frac{\partial \widehat{\mathcal{J}}_{S}}{\partial u_{i}} = -a_{i} \exp\left(-\frac{\zeta}{\tau_{a}}\right) \exp\left(-\frac{u_{i}}{\tau_{a}}\right) + \exp\left(\frac{u_{i}}{\epsilon}\right) \sum_{j=1}^{N} \left[\frac{\exp\left(-\frac{C_{ij}}{\epsilon}\right)}{\sum_{k=1}^{M} \exp\left(\frac{u_{k} - C_{kj}}{\epsilon}\right)}\right] b_{j} = 0.$$

To solve the above problem, we can obtain:

$$u_i^{(l+1)} = \frac{\tau_a \epsilon}{\tau_a + \epsilon} \log \left(a_i \exp\left(-\frac{\zeta}{\tau_a}\right) \right) - \frac{\tau_a \epsilon}{\tau_a + \epsilon} \log \left[\sum_{j=1}^N \left[\frac{\exp\left(-\frac{C_{ij}}{\epsilon}\right)}{\sum_{k=1}^M \exp\left(\frac{u_k^{(l)} - C_{kj}}{\epsilon}\right)} \right] b_j \right]$$
$$= \mathcal{T}(u_i^{(l)}).$$

We can adopt Banach theorem to verify the convergence of the algorithm.

$$\frac{\partial \mathcal{T}(u_i^{(l)})}{\partial u_i^{(l)}} = -\frac{\tau_a \epsilon}{\tau_a + \epsilon} \frac{\frac{\partial}{\partial u_i^{(l)}} \left(\sum_{j=1}^{N} \left[\frac{\exp\left(-\frac{C_{ij}}{\epsilon}\right)}{\sum_{k=1}^{M} \exp\left(\frac{u_k^{(l)} - C_{kj}}{\epsilon}\right)} \right] b_j}{\sum_{j=1}^{N} \left[\frac{\exp\left(-\frac{C_{ij}}{\epsilon}\right)}{\sum_{k=1}^{M} \exp\left(\frac{u_k^{(l)} - C_{kj}}{\epsilon}\right)} \right] b_j}$$

$$= \frac{\tau_a}{\tau_a + \epsilon} \frac{\sum_{j=1}^{N} \left[\frac{b_j \exp\left(-\frac{C_{ij}}{\epsilon}\right)}{\sum_{k=1}^{M} \exp\left(\frac{u_k^{(l)} - C_{kj}}{\epsilon}\right)} \cdot \frac{\exp\left(\frac{u_i^{(l)} - C_{ij}}{\epsilon}\right)}{\sum_{k=1}^{M} \exp\left(\frac{u_k^{(l)} - C_{kj}}{\epsilon}\right)} \right]}{\sum_{j=1}^{N} \left[\frac{\exp\left(-\frac{C_{ij}}{\epsilon}\right)}{\sum_{k=1}^{M} \exp\left(\frac{u_k^{(l)} - C_{kj}}{\epsilon}\right)} \right] b_j}{\sum_{k=1}^{M} \exp\left(\frac{u_k^{(l)} - C_{kj}}{\epsilon}\right)} \right] b_j}$$

$$\leq 1.$$

A.5 IMPLEMENTATION DETAILS

To be fair, we adopt Wide ResNet (WRN) (Zagoruyko & Komodakis, 2016) as the backbone, with WRN-28-2 on CIFAR-10 and WRN-28-8 on CIFAR-100, consistent with the baseline. For each batch, the size of \mathbf{X}_u is twice that of \mathbf{X}_l . Since Fixmatch is used in the closed-set semi-supervised classification module of SDM in the experimental part, we set the temperature parameter of pseudo-label to 1 and the threshold of pseudo-label to 0.95. The model is trained with a Nesterov SGD optimizer with 0.9 momentum and 5×10^{-4} weight decay. We implement the cosine annealing learning rate adjustment strategy and set the initial learning rate as 0.03. τ_a in Equation (2) is set to 0.01 when comparing SDM with baselines. The selection of hyperparameters in MCR refers to (Zhang et al., 2023). Putting all the components together, we set the balance factor of L_x and L_u as 1 while setting that of L_{ood} and L_{mcr} as 0.01. For the ImageNet-30 dataset, We use ResNet-18 (He et al., 2016) as the backbone, the experimental settings are the same as the case on CIFAR-10/100.

A.6 LIMITATIONS

The proposed method has two main limitations as follows:

- 1) Tough the DSA approach does not lead to extra testing latency, the computation of OT or SemiUOT in high-dimensional feature embedding is relatively high in training phase, placing demands on the performance of computing devices. In future work, we will focus on further accelerating it via parallel computing strategy and exploring dimension reduction to low-dimensional space for calculation.
- 2) The pseudo labels obtained during training phase is only used for the supervision of neural networks to perform OOD detection. More efforts can be made to enhance the performance of closed-set classification module via the pseudo labels (e.g., through a joint optimization framework).